RSC Advances

PAPER

View Article Online
View Journal | View Issue

Cite this: *RSC Adv.*, 2020, **10**, 6801

Highly selective colorimetric determination of catechol based on the aggregation-induced oxidase–mimic activity decrease of δ-MnO_2†

Pengyu Xiao,[a] Yang Liu,[a] Wenjing Zong,[a] Jin Wang,*[b] Minghuo Wu,[a] Jingjing Zhan,[a] Xianliang Yi,[a] Lifen Liu[a] and Hao Zhou*[a]

Received 13th December 2019
Accepted 7th February 2020

DOI: 10.1039/c9ra10480a

rsc.li/rsc-advances

Multiple enzyme-like activities of manganese oxides (MnO_2) have been reported and applied in catalysis, biosensors, and cancer therapy. Here, we report that catechol can be determined colorimetrically based on the 3,3′,5,5′-tetramethylbenzidine (TMB) oxidase-like activity of δ-MnO_2. The detection was based on pre-incubation of catechol containing water samples with δ-MnO_2, and then the residual TMB oxidase-like activity of reacted δ-MnO_2 was linearly dependent on the catechol concentration in the range of 0.5 to 10 μM. This determination method was stable at pH 3.73–6.00 and was not affected by ion strength up to 200 μM. Common co-solutes in water bodies (50 μM) have negligible effects and excellent selectivity of catechol among various phenolic compounds (15 μM) was facilitated. Both reduction and aggregation of δ-MnO_2 were observed during the incubation process with catechol, and aggregation-induced TMB oxidase–mimic activity decrease was the main factor for this colorimetric determination.

1. Introduction

Phenolic compounds widely exist in natural water bodies and industrial wastewaters, and exhibit adverse effects on human health and the environment.[1] Among these compounds, catechol has attracted concern because of its widespread occurrence in nature and its potential toxicity to human beings. It is used as an antifungal agent on seed potatoes or as an antioxidant in the rubber, dye, pharmaceutical and oil industries.[2] It is also an important intermediate produced by bacteria during aerobic aromatic compound degradation. For human beings, 50 mg L^{-1} catechol is enough to cause significant changes in erythrocyte function.[3] Herein, a variety of methods, such as UV-vis spectrophotometry, liquid chromatography, electrochemical analysis, and flow injection analysis, have been developed to facilitate catechol determination.[4–8] However, the intrinsic drawbacks, such as complicated instruments, time-consuming pre-treatment, and low determination limits, restrict the practical application of these methods.

In the early decades of the 21st century, unexpected enzyme-like activities of nanomaterials were observed, and those nanomaterials were termed "nanozymes".[9] By employing the peroxidase, catalase, superoxide dismutase, and hydrogenase-like activities of different nanozymes, a variety of analytic platforms have been established through electrochemical and luminescence signal changes induced by substrate concentration.[10–12] MnO_2 is a relatively new type of nanozyme, that was reported to possess oxidase-like activity against 3,3′,5,5′-tetramethylbenzidine (TMB).[13–16] The blue oxidation product of TMB (ox-TMB) has a large molar extinction coefficient of 39 000 M^{-1} cm^{-1} at 652 nm in UV-vis spectra, which makes this oxidation reaction suitable for colorimetric detection.[17] In general, the TMB–MnO_2 system can be applied to quantitatively determine any substrate that can inhibit the oxidase-like activity of MnO_2. The inhibition effect is usually caused by either the redox reaction between the substrate and MnO_2, or the strong absorption of substrate on the surface of MnO_2.[18] In the case of catechol, unfortunately, these two approaches cannot apply enough selectivity and sensitivity because the reaction rate and adsorption capacity of catechol with MnO_2 are not superior to those of other phenolics. Interestingly, reduction-induced MnO_2 aggregation by catechol, guaiacol and 4-methylguaiacol was observed, while 4-methylphenol and *p*-cresol cannot induce MnO_2 aggregation.[19] This phenomenon inspired us to determine whether this "reduction-induced aggregation" can be used for catechol determination with satisfactory selectivity and sensitivity.

In this paper, δ-MnO_2 was synthesized, and its TMB oxidase-like activity was confirmed and optimized. Then, TMB oxidase-like activity was successfully used to determine catechol with good sensitivity and selectivity. This nanozyme-based system also exhibited a reasonable RSD value and recovery ratio in real

[a]*Key Laboratory of Industrial Ecology and Environmental Engineering (Ministry of Education), School of Ocean Science and Technology, Panjin Campus, Dalian University of Technology, 116023, China. E-mail: zhouhao@dlut.edu.cn*

[b]*College of Agriculture and Biology, Shanghai Jiao Tong University, Shanghai, 200240, China. E-mail: wangjin100@sjtu.edu.cn*

† Electronic supplementary information (ESI) available. See DOI: 10.1039/c9ra10480a

water samples. Moreover, an aggregation-based determination mechanism of catechol was proposed.

2. Experimental

2.1 Materials and chemicals

TMB, dopamine (DOPA) and 2,2′-azino-bis(3-ethylbenzothiazoline-6-sulfonic acid) (ABTS) were purchased from Sigma-Aldrich (Steinheim, Germany), and methanol and dimethyl sulfoxide (DMSO) were purchased from Merck (Shanghai, China). All of the other chemicals were of analytical grade and purchased from Damao (Tianjin, China) or Aladdin (Shanghai, China). The metal salts used in this study were all in the chloride form, and the anions were all in the sodium form.

2.2 Synthesis and characterization

Birnessite-type MnO_2 (δ-MnO_2) was obtained through the redox reaction between $KMnO_4$ and methanol, as our previous work mentioned.[20] The products were collected and characterized. The morphology of δ-MnO_2 was observed using transmission electron microscopy (TEM, Tecnai F30, FEI), and the chemical environment and element valences of the material surface were determined by X-ray photoelectron spectroscopy (ESCALAB™ 250Xi). The hydrodynamic radius of nanoparticles was determined by a nano-ZS zetasizer (Malvern, England). The Mn concentration in the solution was determined by atomic absorption spectroscopy (AAS, Techcomp AA6100). The catechol concentration was determined by high-performance liquid chromatography (HPLC, Agilent 1290). A gradient elution method was used for catechol determination. Mobile phase A was ultrapure water, and mobile phase B was acetonitrile. The gradient was as the follows (% B): 0 min (20%), 3 min (95%), 8 min (95%), and 8.1 min (20%). The re-equilibration time was 1.9 min. The flow rate was kept at 0.4 mL min^{-1}.

2.3 TMB oxidase-like activity determination

In general, 5 mg δ-MnO_2 power was added to 25 mL 20 mM HAc–NaAC buffer and sonicated for 5 min to obtain δ-MnO_2 dispersions. Then, 50 μL of these dispersions was added to 1930 μL 20 mM HAC–NaAC buffer in a cuvette. Furthermore, 50 mg TMB was added to 5 mL DMSO to prepare a stock solution of TMB. 20 μL of this stock TMB solution was mixed with the pre-added δ-MnO_2 dispersions and buffer, and reacted for 5 min. The absorbance at 652 nm ($A_{652\ nm}$) was monitored in either fixed wavelength or whole wavelength scanning mode (500 to 800 nm) by a UV-vis spectroscopy (723PC, SOPTOP Co. Ltd., China). To investigate the effect of pH, different buffers were used as follows: HAC–NaAC (pH 3.73 to 5.00, 20 mM), MES (pH 6.00, 20 mM), HEPES (pH 7.00, 20 mM) and Tris–HCl (pH 8.00 to 9.00, 20 mM). The ion strength referred to the concentration of HAc–NaAc buffer. The concentrations of common anions and cations were 50 μM. For the selectivity experiments, all of the phenolic compounds were used at a final concentration of 15 μM.

3. Results and discussion

3.1 TMB oxidase-like activity of δ-MnO_2

The TMB oxidase-like activity of as-synthesized δ-MnO_2 was first determined by UV-vis spectroscopy. As shown in Fig. 1a, $A_{652\ nm}$ increased with the δ-MnO_2 concentration, reaching approximately 1.4 with the addition of 5 mg L^{-1} δ-MnO_2. A further increase in the δ-MnO_2 concentration to 8 mg L^{-1} resulted in the value of $A_{652\ nm}$ increasing to 2.5, which means that dilution of the sample was needed to obtain an accurate value because of the limitation of the Lamber–Bill law. Increase in the TMB concentration first increased $A_{652\ nm}$, with 5 mg L^{-1} TMB giving an $A_{652\ nm}$ of 1.42. Further increase in the TMB concentration resulted in only a slight increase in $A_{652\ nm}$ (Fig. 1b). The oxidation of TMB was fast, and $A_{652\ nm}$ reached a stable value within 300 s (Fig. 1c). The TMB oxidase activity of δ-MnO_2 is highly pH-dependent and maintained a relatively high value between pH 3.73 and 6.00, and then decreased sharply at pH 8.00 (Fig. 1d). This pH-dependent activity has been reported widely and is thought to be related to the oxidation power of MnO_2 itself.[21] Common coexisting cations and anions, together with a range of ion strengths (5 to 200 mM) showed insignificant effects on the TMB oxidase activity (Fig. 1e and f). Therefore, the following experiments were carried out under the following reaction conditions unless otherwise mentioned: [MnO_2] = 5 mg L^{-1}, [TMB] = 5 mg L^{-1}, pH 3.73 (HAc–NaAc buffer), 20 mM NaCl, and a reaction time of 5 min.

3.2 Linearity and sensitivity to catechol determination

Then, different concentrations of catechol solution were mixed with δ-MnO_2 dispersions, and TMB was added to this solution to determine the residual TMB oxidase activity immediately. It was found that adding catechol has a negligible effect on the TMB oxidation activity. However, if catechol was pre-incubated with δ-MnO_2 for 2 h and then reacted with TMB for 5 min, a significant decrease in $A_{652\ nm}$ was observed, and 15 μM catechol completely quenched the oxidase-like activity of δ-MnO_2 (Fig. 2a). The color change from bright blue to colorless could be observed by the naked-eye when the catechol concentration increased from 0 to 15 μM (Fig. 2b). The $\Delta A_{652\ nm}$ was linearly related to the catechol concentration in the range of 0.5 to 10 μM, with a calculated limit of determination (LOD) of 218 nM (n = 11) and limit of quantification (LOQ) of 726 nM (Fig. 2c). Electrochemical and fluorescence-based determination methods usually have higher sensitivities than colorimetric-based methods, but the instruments are more expensive than that needed for UV-vis spectroscopy.[22,23] However, the performance of TMB-δ-MnO_2 for catechol determination is comparable to most of the reported catechol sensors, as summarized in Table 1. In addition to TMB, DOPA and ABTS were also employed to test the oxidase-like activity of δ-MnO_2. DOPA is a specific oxidase substrate for CeNPs and cannot be oxidized by as-synthesized δ-MnO_2.[24] ABTS, however, can also be effectively oxidized by δ-MnO_2 like TMB and forms a dark green product (Fig. 2d and e). The linear range was 0.5 to

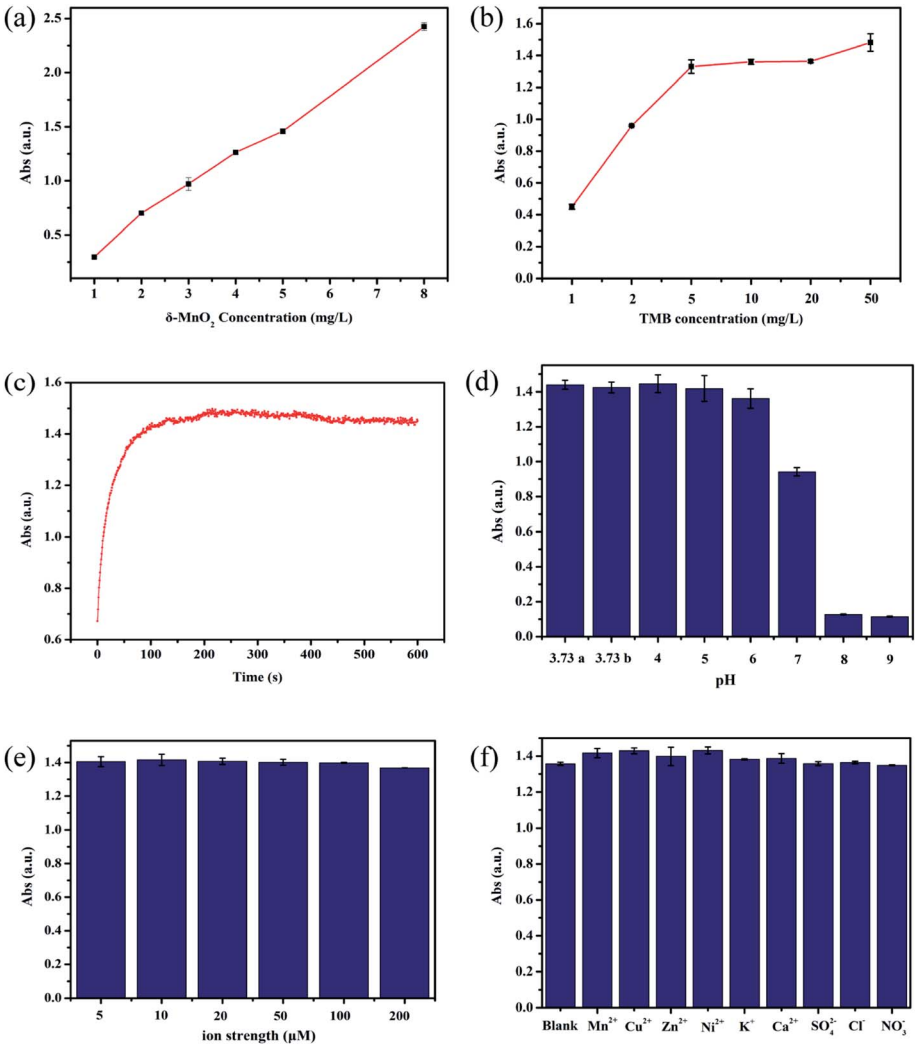

Fig. 1 Effects of a variety of factors on the TMB oxidase-like activity of δ-MnO_2. (a) Effect of δ-MnO_2 concentration. (b) Effect of TMB concentration. (c) Effect of reaction time. (d) Effect of pH. 3.72a was assayed in 100 mM NaCl, while 3.72b was assayed in HAC–NaAC buffer. (e) Effect of ion strength. (f) Effect of common anions and cations.

10 μM, with a calculated LOD of 190 nM ($n = 11$) and LOQ of 577 nM (Fig. 2f).

3.3 Selectivity and practical application

Considering that the colorimetric determination procedure involves a relatively long pre-incubation process between the catechol-containing solution and δ-MnO_2, the effects of pH, cations and anions, incubation time, and ion strength on the final TMB oxidation activity (*i.e.*, $A_{652\ nm}$) were also investigated. The $A_{652\ nm}$ remained stable when the pH was between 3.73 and 6.00 in the presence of various ions, regardless of the ion strength (5–200 mM) (Fig. S1†). However, the incubation time of catechol and δ-MnO_2 has a great effect on $A_{652\ nm}$ (Fig. 3a). For 10 μM catechol, the $A_{652\ nm}$ decreased nearly linearly with incubation time within 120 min, and then decreased more slowly with prolonged incubation. Therefore, 120 min was sufficient to obtain satisfactory sensitivity. To investigate selectivity, several phenolic compounds were incubated with δ-MnO_2 separately in a similar way as catechol and tested for the corresponding TMB oxidation activity. δ-MnO_2-TMB has at least a 3-fold higher response for catechol than the other phenolic compounds at pH 3.73 (Fig. 3b). The selectivity can be further improved by adjusting the solution pH to 6.00. Under this condition, the catechol response of δ-MnO_2-TMB is at least 160-fold higher than that of the other compounds, demonstrating the high selectivity for catechol (Fig. 3c). The reductive compounds, including ascorbic acid, glutathione and H_2O_2, can also lead the decrease of $A_{652\ nm}$ due to their redox reaction with δ-MnO_2 (Fig. S2†). However, they are unlikely existed in wastewater in aerobic conditions. Therefore, they may not interfere the practical catechol determination. The reproducibility of δ-MnO_2-TMB was also examined by randomly selecting two catechol concentrations to carry out multiple measurements ($n = 8$). The relative standard deviations (RSDs) for the determination of 5 μM and 10 μM catechol was 4.96% and 4.42%, respectively. Moreover, the application of δ-MnO_2-TMB for

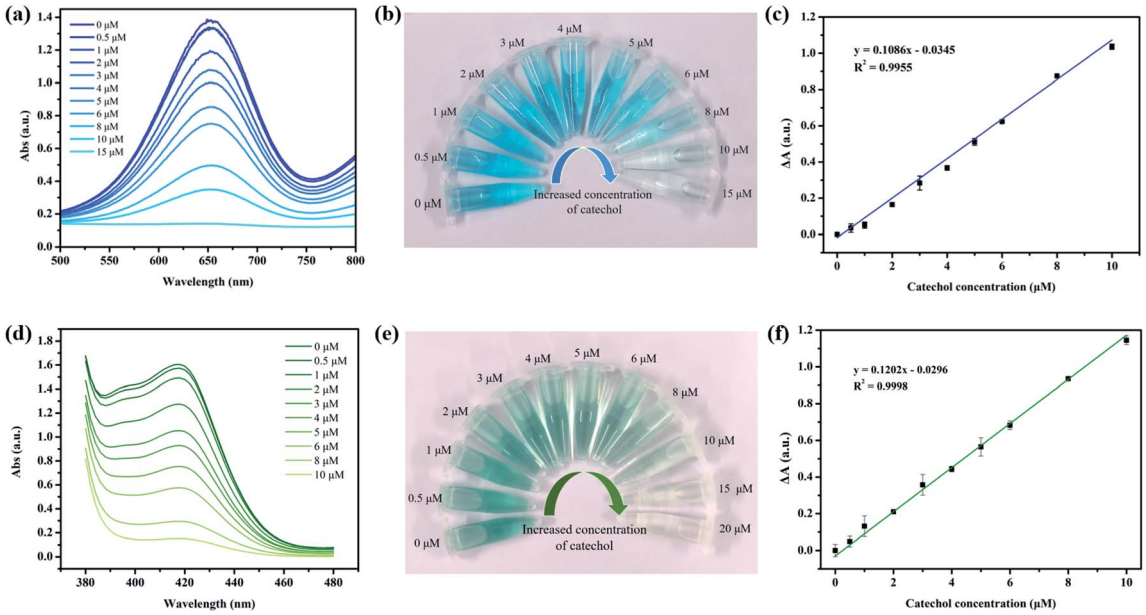

Fig. 2 (a) UV-vis absorption spectra of the resulting solution upon sequential addition of δ-MnO_2 pre-incubated with different concentrations of catechol and TMB. (b) The color change of δ-MnO_2 incubated with different concentrations of catechol and then reacted with TMB. (c) Catechol calibration curve using TMB as the substrate. (d) UV-vis absorption spectra of δ-MnO_2 pre-incubated with different concentrations of catechol and ABTS. (e) The color change of δ-MnO_2 incubated with different concentrations of catechol and then reacted with ABTS. (f) Catechol calibration curve using ABTS as the substrate.

catechol determination in real water samples was also attempted. The recovery ratios of catechol in tap water, reuse water and river water are shown in Table 2, with small RSD values (less than 10.00%) and good recovery (94.80% to 99.56%).

3.4 Determination mechanism

After confirming the excellent sensing performance of δ-MnO_2-TMB to catechol, the sensing mechanism of this system was investigated. The effect of δ-MnO_2 on catechol, *i.e.*, oxidant or catalyst, is still contentious.[19,28] As shown in Fig. 4a, 42.3% of the catechol was quickly removed within the first 5 min, and then a slower increase in removal proportion was observed from 5 to 120 min. The final catechol removal rate was 70%. If ascorbic acid was used as the reaction quencher instead of filtration, the catechol absorbed on the surface of δ-MnO_2 was released again into the solution. By comparing these two removal curves, it can be inferred that pre-absorption of catechol is necessary for its reaction, and absorption is much faster than the reaction. For MnO_2, approximately 8.9% of Mn(II) in MnO_2 was leached during the incubation process, which indicated that a redox reaction occurred between catechol and MnO_2. In other words, δ-MnO_2 is an oxidant for catechol, not a mimic of catechol oxidase.[29] This result is also supported by the XPS spectra and TEM results (Fig. 4b and S3†). The average oxidation state (AOS) of Mn was calculated based on the Mn 3s spectra.[30] After reacting with catechol for 2 h, the AOS of Mn decreased from 3.67 to 3.14, indicating the Mn(IV) and Mn(III) in MnO_2 were reduced to Mn(II). In general, the inhibition of TMB oxidase-like activity of MnO_2 by different compounds (GSH and ascorbic acid) is due to the decomposition of MnO_2, which decrease the amount of MnO_2 significantly.[13,31] However, the small amount of Mn(II) leaching determined by AAS means the mass loss of δ-MnO_2 was less than 10%. Therefore, the redox reaction between catechol and δ-MnO_2 should not be the main factor for the inactivation of TMB oxidase-like activity. Furthermore, the size-dependent activity of nanozymes (Au NPs and Fe_3O_4 NPs) has been reported, but not mentioned in MnO_2-based nanozymes.[32] Fig. 4c shows the DLS results of δ-MnO_2

Table 1 Comparison of the catechol determination methods

Method	System	LOD (μM)	Linear range (μM)	Ref.
Colorimetric	ssDNA-AuNPs	0.11	0.2–7	25
Electrochemical	Fe_3O_4-GO-AuNPs	0.8	2–145	5
Electrochemical	Palygorskite-CPE	0.57	5–100	7
Electrochemical	Array BDD	1.5	5–100	26
Fluorescence	$[C_3(Amp)_2][OH]_2$	0.4	1–1000	27
Colorimetric	TMB-δ-MnO_2	0.22	0.5–10	This work

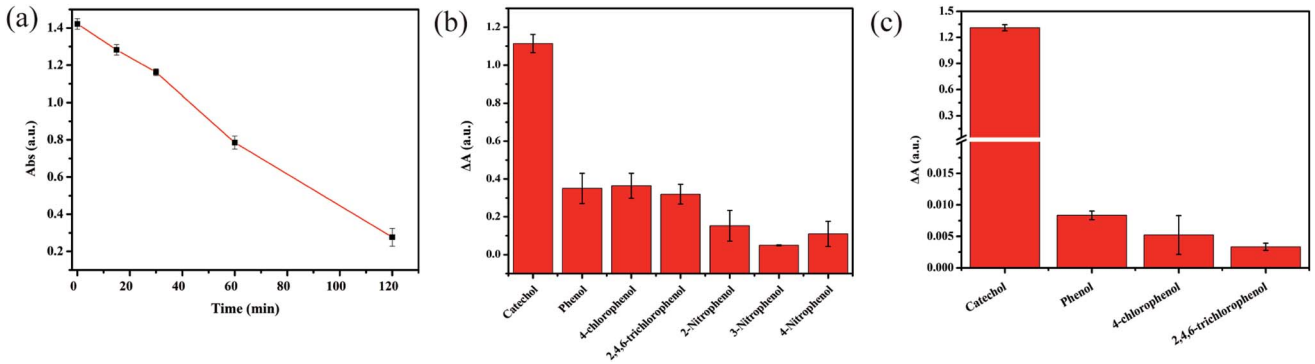

Fig. 3 (a) The effect of incubation time of catechol and δ-MnO_2 (b) detection selectivity of δ-MnO_2-TMB to different phenolic compounds at pH 3.73 (c) detection selectivity of δ-MnO_2-TMB to different phenolic compounds at pH 6.00.

Table 2 Determination of catechol in real water samples using δ-MnO_2-TMB

Water sample	Catechol added (μM)	Catechol found (μM)	RSD (%)	Recovery (%)
Tap water	4.00	3.85	5.62	96.38
	10.00	9.85	3.81	98.50
Reuse water	4.00	3.79	9.96	94.80
	10.00	9.96	2.80	99.56
River water	4.00	3.94	5.61	95.22
	10.00	9.89	1.75	98.92

with different concentrations of catechol. In the absence of catechol, the hydrodynamic radius of MnO_2 was approximately 272.6 ± 20 nm at pH 3.73. Adding 2 μM catechol can induce the aggregation of δ-MnO_2 and increase the hydrodynamic radius of δ-MnO_2 to 488.5 ± 35.67 nm. Adding 10 μM catechol increased the diameter of δ-MnO_2 beyond 10 μm, thus greatly decreasing the TMB oxidase-like activity. As the TMB-δ-MnO_2 showed higher catechol selectivity to the other phenolic substrates at pH 6.00, the hydrodynamic radius of δ-MnO_2 after incubation with 10 μM catechol and *p*-chlorophenol was compared. It can be observed that adding catechol increased the particle size to above 10 μm, while adding the same concentration of *p*-chlorophenol showed slight effect on the hydrodynamic radius of δ-MnO_2. Therefore, catechol-induced δ-MnO_2 specific aggregation should be the key factor in facilitating the sensitive and selective catechol determination. The aggregation mechanism of MnO_2 caused by organics has been reported previously.[19] The organics first reacted with MnO_2 and dissolved MnO_2 to release Mn(II); then, part of the Mn(II) was absorbed on the surface of MnO_2 and formed a complex with the organics. Catechol is a strong complex of Mn(II) and Mn(III). Its oxidation products by δ-MnO_2, *i.e.*, semiquinone and hydroxylated semiquinone, are also strong complexes of Mn(II) and Mn(III), and can form an organic coating on the surface of MnO_2.[33] These organic coatings can act as bridge molecules to induce MnO_2 aggregation.

4. Conclusion

In conclusion, a TMB oxidase-like activity-based detection method for catechol was developed in this study. Catechol was first incubated with δ-MnO_2 for 2 h to induce the δ-MnO_2 aggregation, and then the aggregated δ-MnO_2 reacted with TMB at a much lower rate than the well-dispersed δ-MnO_2. This method has high sensitivity (with an LOD of 218 nM), and high selectivity (160-fold higher than those of other phenolic compounds) for catechol determination. It was also insensible to changes in ion strength and co-existing anions and cations. The only concern is the pH-dependent activity, which made a pre-adjustment of pH into 3.73 to 6.00 necessary for catechol

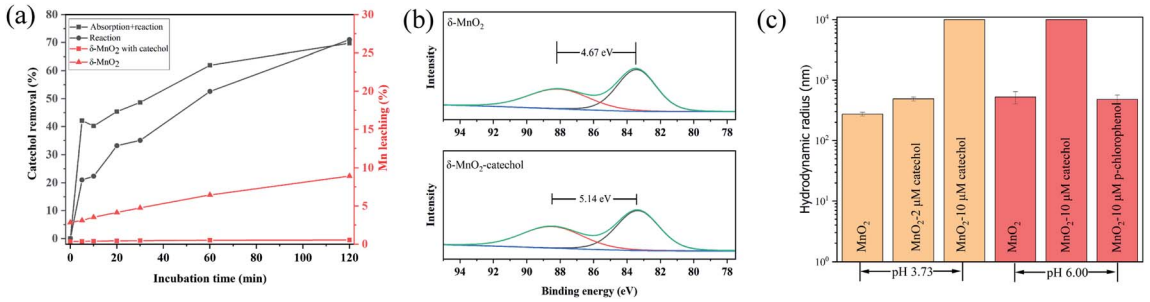

Fig. 4 (a) Catechol removal and Mn(II) leaching profiles during the incubation process. The initial amount of MnO_2 was 50 mg L^{-1}, and the catechol was 150 μM (b) Mn 3s spectra of the pristine δ-MnO_2 and catechol reacted δ-MnO_2. (c) DLS results of pristine δ-MnO_2, and δ-MnO_2 treated with catechol and *p*-chlorophenol.

determination in real water samples. Overall, the reduction-induced aggregation of a nanozyme was first used for the colorimetric determination of pollutants, which provides a new way to modulate and apply the activity of nanozymes.

Conflicts of interest

There are no conflicts to declare.

Acknowledgements

The authors were financially supported by the National Natural Science Foundation of China (Grant No. 41977197) and the Guangxi Major Project of Science and Technology (Grant No. AA17202032, AA18118013) from the Guangxi Science and Technology Department.

References

1 W. Gernjak, T. Krutzler, A. Glaser, S. Malato, J. Caceres, R. Bauer and A. R. Fernández-Alba, *Chemosphere*, 2003, **50**, 71–78.
2 N. Schweigert, A. J. Alexander and R. I. Eggen, *Environ. Microbiol.*, 2001, **3**, 81–91.
3 B. Bukowska and S. Kpwalska, *Toxicol. Lett.*, 2004, **152**, 73–84.
4 H. Du, J. Ye, J. Zhang, X. Huang and C. Yu, *J. Electroanal. Chem.*, 2011, **650**, 209–213.
5 S. Erogul, S. Z. Bas, M. Ozmen and S. Yildiz, *Electrochim. Acta*, 2015, **186**, 302–313.
6 C. Bu, X. Liu, Y. Zhang, L. Li, X. Zhou and X. Lu, *Colloids Surf., B*, 2011, **88**, 292–296.
7 Y. Kong, X. Chen, W. Wang and Z. Chen, *Anal. Chim. Acta*, 2011, **688**, 203–207.
8 J. T. Han, K. J. Huang, J. Li, Y. M. Liu and M. Yu, *Colloids Surf., B*, 2012, **98**, 58–62.
9 L. Gao, J. Zhuang, L. Nie, J. Zhang, Y. Zhang, N. Gu, T. Wang, J. Feng, D. Yang, S. Perrett and X. Yan, *Nat. Nanotechnol.*, 2007, **2**, 577.
10 H. Deng, S. He, X. Lin, L. Yang, Z. Lin, R. Chen, H. Peng and W. Chen, *Chin. Chem. Lett.*, 2019, **30**, 1659–1662.
11 M. Liu, Z. Li, Y. Li, J. Chen and Q. Yuan, *Chin. Chem. Lett.*, 2019, **30**, 1009–1012.
12 J. Zheng, D. Song, H. Chen, J. Xu, N. S. Alharbi, T. Hayat and M. Zhang, *Chin. Chem. Lett.*, 2019, DOI: 10.1016/j.cclet.2019.09.037.
13 J. Liu, L. Meng, Z. Fei, P. J. Dyson, X. Jing and X. Liu, *Biosens. Bioelectron.*, 2017, **90**, 69–74.
14 X. Liu, Q. Wang, H. Zhao, L. Zhang, Y. Su and Y. Lv, *Analyst*, 2012, **137**, 4552–4558.
15 J. Ge, R. Cai, X. Chen, Q. Wu, L. Zhang, Y. Jiang, C. Cui, S. Wan and W. Tan, *Talanta*, 2019, **195**, 40–45.
16 L. He, F. Wang, Y. Chen and Y. Liu, *Luminescence*, 2018, **33**, 145–152.
17 A. Roy, R. Sahoo, C. Ray, S. Dutta and T. Pal, *RSC Adv.*, 2016, **6**, 32308–32318.
18 L. Lin, D. Shi, Q. Li, G. Wang and X. Zhang, *Anal. Methods*, 2016, **8**, 4119–4126.
19 X. Huangfu, J. Jiang, J. Ma, Y. Wang, Y. Liu, X. Lu, X. Zhang and H. Cheng, *Colloids Surf., A*, 2015, **482**, 485–490.
20 Y. Liu, H. Zhou, R. Cao, X. Liu, P. Zhang, J. Zhang and L. Liu, *Appl. Catal., B*, 2019, **245**, 569–582.
21 C. K. Remucal and M. Ginder-Vogel, *Environ. Sci.: Processes Impacts*, 2014, **16**, 1247–1266.
22 M. Li, X. Huang and H. Yu, *Mater. Sci. Eng., C*, 2019, **101**, 614–618.
23 R. Ai and Y. He, *Sens. Actuators, B*, 2020, **304**, 127372.
24 A. Asati, S. Santra, C. Kaittanis, S. Nath and J. M. Perez, *Angew. Chem., Int. Ed. Engl.*, 2009, **48**, 2308–2312.
25 L. P. Zhang, Y. P. Xing, L. H. Liu, X. H. Zhou and H. C. Shi, *Sens. Actuators, B*, 2016, **225**, 593–599.
26 M. Lv, M. Wei, F. Rong, C. Terashima, A. Fujishima and Z. Z. Gu, *Electroanalysis*, 2010, **22**, 199–203.
27 S. K. Patil, S. A. Patil, M. M. Vadiyar, D. V. Awale, A. S. Sartape, L. S. Walekar, G. B. Kolekar, U. V. Ghorpade, J. H. Kim and S. S. Kolekar, *J. Mol. Liq.*, 2017, **244**, 39–45.
28 A. Naidja and P. M. Huang, *Surf. Sci.*, 2002, **506**, 243–249.
29 Y. Liu, H. Wu, Y. Chong, W. G. Wamer, Q. Xia, L. Cai, Z. Nie, P. Fu and J. Yin, *ACS Appl. Mater. Interfaces*, 2015, **7**, 19709–19717.
30 J. Nie and H. Liu, *J. Catal.*, 2014, **316**, 57–66.
31 W. Huang, Y. Deng and Y. He, *Biosens. Bioelectron.*, 2017, **91**, 89–94.
32 M. Kalantari, T. Ghosh, Y. Liu, J. Zhang, J. Zou, C. Lei and C. Yu, *ACS Appl. Mater. Interfaces*, 2019, **11**, 13264–13272.
33 A. Naidja, P. M. Huang and J. M. Bollag, *Soil Sci. Soc. Am. J.*, 1998, **62**, 188–195.

